Transformation of Human Osteoblast Cells to the Tumorigenic Phenotype by Depleted Uranium-Uranyl Chloride

Alexandra C. Miller,[1] William F. Blakely,[1] David Livengood,[1] Tim Whittaker,[1] Jiaquan Xu,[1] John W. Ejnik,[1] Matthew M. Hamilton,[1] Eric Parlette,[1] Theodore St. John,[2] Henry M. Gerstenberg,[2] and Hannah Hsu[3]

[1]Applied Cellular Radiobiology Department and [2]Radiation Sciences Department, Armed Forces Radiobiology Research Institute, Bethesda, MD 20889-5603 USA; [3]Molecular Pharmacology Branch, Division of Cancer Treatment, National Cancer Institute, National Institutes of Health, Bethesda, MD 20892 USA

Depleted uranium (DU) is a dense heavy metal used primarily in military applications. Although the health effects of occupational uranium exposure are well known, limited data exist regarding the long-term health effects of internalized DU in humans. We established an *in vitro* cellular model to study DU exposure. Microdosimetric assessment, determined using a Monte Carlo computer simulation based on measured intracellular and extracellular uranium levels, showed that few (0.0014%) cell nuclei were hit by alpha particles. We report the ability of DU-uranyl chloride to transform immortalized human osteoblastic cells (HOS) to the tumorigenic phenotype. DU-uranyl chloride-transformants are characterized by anchorage-independent growth, tumor formation in nude mice, expression of high levels of the k-*ras* oncogene, reduced production of the Rb tumor-suppressor protein, and elevated levels of sister chromatid exchanges per cell. DU-uranyl chloride treatment resulted in a 9.6 (± 2.8)-fold increase in transformation frequency compared to untreated cells. In comparison, nickel sulfate resulted in a 7.1 (± 2.1)-fold increase in transformation frequency. This is the first report showing that a DU compound caused human cell transformation to the neoplastic phenotype. Although additional studies are needed to determine if protracted DU exposure produces tumors *in vivo*, the implication from these *in vitro* results is that the risk of cancer induction from internalized DU exposure may be comparable to other biologically reactive and carcinogenic heavy-metal compounds (e.g., nickel). *Key words*: alpha radiation, depleted uranium, osteoblast, transformation. *Environ Health Perspect* 106:465–471 (1998). [Online 6 July 1998] *http://ehpnet1.niehs.nih.gov/docs/1998/106p465-471miller/abstract.html*

Several U.S. military personnel participating in Operation Desert Storm were wounded in friendly fire accidents and have retained large fragments (approximately 2–20 mm) of depleted uranium (DU) in their bodies. DU, used in military munitions in the United States, was shown to be an effective material in kinetic energy penetrators in the 1991 Persian Gulf War. Chemically similar to natural uranium (*1*), DU is a low specific-activity heavy metal, with a density approximately 1.7 times that of lead (19 g/cm^3 versus 11.35 g/cm^3). DU differs from natural uranium in that it has been depleted of ^{235}U and ^{234}U. As a result, the specific activity of DU is significantly lower than that of natural uranium (0.4 µCi/g versus 0.7 µCi/g, respectively) (*2*).

Assessment of the carcinogenic risks from DU is complicated by the dual toxicity of uranium (i.e., chemical as well as radiological). Epidemiological studies have linked uranium mining and milling to human carcinogenesis (*1*), but there are no published studies to permit an accurate assessment of risks for carcinogenesis from DU. The radiological health risks (external exposure) to personnel handling DU munitions were evaluated and determined to be within allowed occupational exposure limits (*1,2*); the health risks from internalized DU, however, are more difficult to estimate due to the physical and chemical properties of the internalized DU (*3*). The chemical toxicity of acute, short-term exposures to uranium, primarily manifested as renal, pulmonary, and developmental toxicity, has clearly been demonstrated in animals and humans (*4*). In contrast, the long-term health risks associated with internal chronic exposure are not as clearly defined (*1*). In view of carcinogenesis risk estimates and medical management questions relevant to current and possible future incidents of DU internalization, an examination of molecular and cellular effects, including the potential transforming ability of DU, are necessary to understanding the potential carcinogenic effects of DU. The use of cell culture models to investigate potential or known carcinogens can provide important insights into the cellular and molecular mechanisms of carcinogenesis.

In spite of epidemiological studies that suggest that uranium is a carcinogen (*1*), there is no evidence that uranium of any type (depleted, naturally occurring, or enriched) can transform human cells to the tumorigenic phenotype (*1*). Furthermore, the *in vitro* transformation assay has not previously been used to study the transforming ability of any uranium compounds (depleted, naturally occurring, or enriched uranium). This assay has been widely used in conjunction with metal salts to assess the potential carcinogenicity of metal compounds (e.g., nickel, chromium, lead) (*5–8*) and therefore we chose to use this assay to assess the potential carcinogenicity of DU. Investigations using metal salts have also been able to clarify the contradictions observed in some animal and human carcinogenicity studies (*8*). The HOS TE85 cell line, an immortalized, nontumorigenic osteoblastlike cell line, has been successfully used to demonstrate the transformation of nontumorigenic human cells to the tumorigenic phenotype by metals (*7,8*) and chemical (*9*) carcinogens. We chose the DU compound DU-UO_2Cl_2, which readily forms the UO_2^{2+} cation in solution, as the depleted uranium metal salt to be tested. We used nickel sulfate and lead acetate, which have previously been shown to transform cells *in vitro*, for comparison.

Our data demonstrate for the first time that a DU compound can transform human cells to the tumorigenic phenotype, similar to results observed with some nickel compounds (*6–8*). Isolated DU transformants form anchorage-independent colonies, produce tumors when injected into athymic mice, express the k-*ras* oncogene, and have an altered phosphorylation of the Rb tumor-suppressor protein. Based on these *in vitro* results, the carcinogenic potential of internalized DU remains a concern and warrants additional studies with experimental animals.

Materials and Methods

Cell lines and culture. Human osteosarcoma cell lines HOS (TE85, clone F-5) were obtained from the American Type Culture Collection (Rockville, MD). Cell cultures

Address correspondence to A.C. Miller, Applied Cellular Radiobiology Department, Armed Forces Radiobiology Research Institute, 8901 Wisconsin Avenue, Bethesda, MD 20889-5603 USA.

The contributions of Eric Daxon, David McClain, John Kalanich, C. Robert Woodruff, Ramesh Bhatt, Gerald Vavrina, Christopher Pitcher, and Betty Ann Torres are greatly appreciated and were invaluable to the success of this project.

This research was supported in part by the Armed Forces Radiobiology Research Institute under work unit numbers AFRRI-98-3 and AFRRI-98-4. The views presented are those of the authors and do not reflect the official views of the Department of Defense or the U.S. government.

Received 7 November 1997; accepted 11 March 1998.

were propagated in Dulbecco's modified Eagle medium (D-MEM) supplemented with 2 mM glutamine, 10% heat-inactivated fetal calf serum (Gibco Laboratories, Grand Island, NY), 100 U/ml penicillin, and 100 µg/ml streptomycin (Sigma, St. Louis, MO). Cells were tested for mycoplasma by MycoTect Kit (Sigma), and only cells negative for mycoplasma were used.

Transformation and cell growth studies. DU-UO_2Cl_2 was initially dissolved in sterile water (freely soluble in water). Based on previous unpublished work with uranyl compounds which demonstrated that micromolar concentrations are relatively nontoxic to cultured cells, we chose a concentration of 10 µM for transformation and cell growth studies. Metal salts were added to sterile water and then filtered to prepare concentrated stock solutions that were used throughout these studies. Dilutions from concentrated stock solutions were dissolved into complete medium immediately before exposure. Briefly, 1×10^6 cells were treated with DU-UO_2Cl_2 (10–250 µM), $NiSO_4$ (10 µM), or lead acetate (10 µM) for 24 hr in complete medium. After treatment, cells were rinsed, trypsinized, counted, and seeded in 100-mm tissue culture dishes at a density calculated to yield about 125–225 surviving cells per dish. Approximately 150 replicate dishes were seeded for each treatment group. The cultures were incubated for 5 weeks with weekly changes of nutrient medium.

For quantitative transformation assessment, at the end of the incubation period, cells were fixed, stained, and examined for the appearance of transformed foci (*10*). We assayed transformed foci using the criteria developed by Reznikoff et al. (*10*) and the IARC/NCI/EPA Working Group (*11*). The working group report indicated that because of the continuum of focus morphology, some foci can be intermediate (I/II, II/III) in character, and these foci should be scored conservatively and assigned to the category of lower aggressive behavior. With the HOS cells it was easy to distinguish between a type I and a type II foci, but somewhat difficult to differentiate between type II and type III foci. Therefore, in our experiments, only type II and type II/type III foci were scored as transformants. In Table 1, number of dishes with foci equals number of foci of type II plus type III. Details of the transformation frequency calculations and the standard error were described elsewhere (*12*) but are outlined below. Transformed foci are not contact inhibited and may be dislodged during refeeding forming satellite colonies. To avoid this source of errors, the average number of transformed foci per dish, λ, was computed from the proportion of dishes free of transformed colonies, f, i.e., $\lambda = -\ln f$. To determine the transformation frequency, the following formula was used:

$$\text{Transformation frequency} = \lambda/\text{number of surviving cells per dish}$$

This calculation has been widely used in radiation-induced neoplastic transformation studies to quantitatively compare transformation frequencies. The transformation data are presented from three independent experiments unless otherwise noted.

We determined cell survival fraction (SF) using the conventional clonogenic assay (*9*). Cytotoxicity and survival assays were conducted in parallel with each transformation assay as described (*9*). Several transformed foci were picked by cloning cylinders and expanded by mass culture to establish transformed clonal lines. The transformation dose–response curve was determined as indicated above, except that increasing concentrations of DU-UO_2Cl_2 were used. We selected the optimal dose level for transformation following a preliminary toxicity test based upon colony-forming efficiency. The high dose selected resulted in >90% toxicity, and the low dose selected resulted in minimal toxicity. Three intermediate doses were also selected.

To determine saturation densities, cells were plated at 1×10^5 cells per 100-mm diameter plate in complete growth medium and monitored for growth as previously described (*9*). For the soft-agar clonability assay, cells were plated at a density of 2×10^3 cells per well in a six-well plate sandwiched by 1-ml bottom agar (0.6%) and 1-ml top agar (0.3%). Cells were fed weekly by adding a new layer of top agar. Colonies >0.5-mm diameter were scored using a microscope after 2 weeks. The plating efficiency value for each clone represents the mean number of colonies scored from three wells. For both saturation density determination and plating efficiency in soft agar, data represent three independent experiments.

Tumorigenicity assay. Experiments were performed with 4- to 5-week-old female athymic mice (Division of Cancer Treatment, NCI Animal Program, Frederick Cancer Research Facility). For this assay, 5×10^6 or 1×10^6 cells in a 0.2-ml sterile suspension were injected subcutaneously in the right scapula. Animals were then observed for tumor growth at the sites of injection. The appearance of tumor growth was monitored daily for 180 days. Tumor area was measured using a caliper measurement of two perpendicular diameters. When tumors were >100 mm^2, the animal was euthanized.

Sister chromatid analysis. The yield of sister chromatid exchange (SCE) per cell in control and DU-UO_2^{2+} exposed cells following a 24-hr exposure was assessed in 100 second mitotic metaphase spreads (48-hr culture) using the conventional fluorescence-plus-Giemsa harlequin staining protocol (*13*). The SCE yield in selected transformed clones was similarly determined.

Microdosimetry. The term "specific energy" is used rather than "dose" because dose refers to macroscopic averages, whereas specific energy is a microdosimetric equivalent (i.e., dose to a single cell). We applied microdosimetric methods using Monte Carlo computer simulations (*14*). The code

Table 1. Morphological transformation of human osteoblastlike cells by depleted uranium-uranyl chloride: comparison to nickel sulfate and lead acetate

Metal	Concentration (µM)	Surviving fraction	Survivors/ dish	No. of dishes	No. dishes with type II or type II/III foci	No. of dishes without foci	λ	Transformation frequency per survivor[a] × 10^{-4}
Experiment 1								
None	0	1.0	201	155	13	142	0.084	4.2 ± 1.1
DU-uranyl chloride	10	0.95	122	165	64	101	0.491	40.2 ± 5.0
Nickel sulfate	10	0.97	116	150	40	110	0.312	26.9 ± 3.4
Lead acetate	10	0.99	119	150	31	119	0.237	19.9 ± 2.3
Experiment 2								
None	0	0.99	180	141	12	129	0.088	4.9 ± 1.1
DU-uranyl chloride	10	0.96	101	110	40	70	0.448	44.4 ± 5.1
Nickel sulfate	10	0.97	110	122	35	87	0.337	30.7 ± 3.7
Lead acetate	10	0.97	107	127	25	102	0.219	20.5 ± 2.9
Experiment 3								
None	0	0.99	149	140	9	131	0.066	4.24 ± 1.0
DU-uranyl chloride	10	0.96	115	120	47	73	0.490	42.6 ± 5.2
Nickel sulfate	10	0.98	115	120	32	88	0.320	27.5 ± 2.6
Lead acetate	10	0.96	114	120	26	94	0.251	22.3 ± 2.7

[a]The transformation data illustrated are from three independent experiments involving approximately 400 plates/metal. Transformed foci were assayed according to the criteria of Reznikoff et al. (*10*) with type II and type III foci being scored as transformants. Therefore, the "dishes with foci" values shown include only those colonies that were morphologically consistent with either type II or type III foci as described by Reznikoff et al. The average number of transformed foci per dish was computed from the proportion of dishes free of transformed colonies, f, by $\lambda = -\ln f$. Transformation frequency = λ/number of surviving cells per dish (*12*).

was modified to include the following parameters in the calculations: cell location and size, distribution of uranium (intracellular and extracellular), specific activity, alpha particle energies, media volume, and molar concentration of uranyl chloride. We calculated the trajectory of each alpha particle using vector analysis to determine whether it would hit a nucleus. For those that scored a hit, the amount of energy transferred to the nucleus was calculated by determining the residual energy retained by the alpha particle as it penetrated the nucleus and integrating the fractional energy loss under the Bragg curve from the entry point to the exit point.

Kinetic phosphorescence analysis of uranium. Kinetic phosphorimetry measurements were performed using a kinetic phosphorescence analyzer (KPA) (*15*). To determine the amount of uranium per cell following a 24-hr treatment with 10 µM DU-UO_2^{2+}, cells were treated and then rinsed in phosphate-buffered saline. Using previously described procedures, cells were lysed and fractionated into subcellular fractions. Lysates were analyzed for uranium content as described (*15*).

Northern blot analysis and DNA probes. Cytoplasmic RNA was extracted from exponentially growing cells and separated by electrophoresis in 1% agarose-formaldehyde gels. RNA preparation and blotting onto nytran filters, hybridization with radiolabeled DNA probes, and autoradiography were as previously described (*9*). The *ras* probe, a Sac I 2.9 kb fragment of the human k-*ras* gene, was obtained from Oncor (Gaithersburg, MD). We prepared ^{32}P-labeled DNA probes using a random primed DNA labeling kit (Boehringer Mannheim, Germany).

Metabolic labeling and immunoprecipitation of pRb. Exponentially growing cells [1 × 10^6 per T75-cm^2 flask (Costar)] were radiolabeled with ^{32}P-orthophosphate (250 µCi) for 24 hr and lysed in buffer (1% Triton X-100, 0.05 M Tris-HCl, pH 8.0, 5 mM $MgCl_2$ and 0.1 M NaCl). Lysates were incubated with polyclonal anti-pRb antibody-agarose conjugates (Oncogene Science, NY) for 2 hr at 4°C. Processing of immunoprecipitates was as previously described (*9*). The proteins were resolved on 7.5% polyacrylamide gels and analyzed by autoradiography.

Results

Characterization of model system: cytotoxicity, SCE induction, and microdosimetry. We initially assessed the effect of DU-UO_2CL_2 exposure on cell growth and survival, cytogenetic damage, and microdosimetry to characterize our cell model system. No effect on cell survival (surviving fraction, SF, 0.96 ± 0.04) was observed using the standard colony formation assay (*9*) following a 24-hr exposure to DU-UO_2^{2+} (10 µM). Growth rate analysis by cell enumeration and thymidine incorporation into DNA (*9*) similarly revealed that the DU-UO_2^{2+} treatment did not affect cell growth during the 24-hr exposure (inhibitory concentration, IC_{50}, 45 µM). Therefore, to preclude excessive cell killing due to heavy metal toxicity, the nontoxic, noncytostatic concentration chosen for the transformation experiment was 10 µM (24-hr exposure). The colony formation assay was also used to assess the cytotoxicity of $NiSO_4$ and lead acetate. Similarly, nontoxic concentrations of $NiSO_4$ and lead acetate were chosen (20 µM, SF = 0.94; 20 µM, SF = 0.095, respectively).

Cytogenetic analysis of the acute effect of the 24-hr exposure to 10 µM DU-UO_2^{2+} was assessed in the *in vitro* HOS model system using the SCE assay. As seen in Figure 1A, this acute DU exposure caused an approximately twofold increase in SCE induction (untreated: 8.3 SCE/cell; DU-UO_2^{2+}: 17.9 SCE/cell). In comparison, lead acetate treatment did not result in a significant increase in SCEs, while nickel did induce a small but significant increase

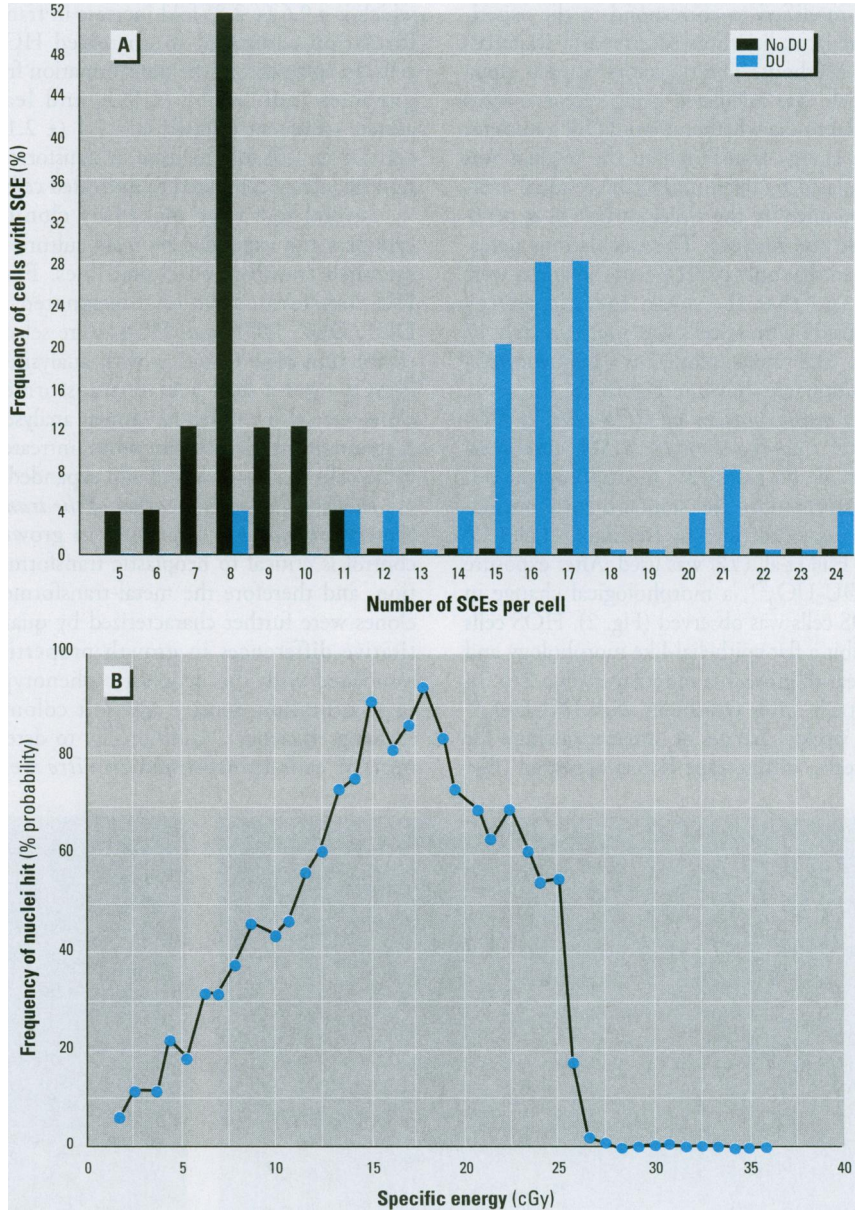

Figure 1. Characterization of an *in vitro* HOS cellular model to access DU-UO_2^{2+} exposure. The effect of DU-UO_2^{2+} exposure (24 hr, 10 µM) on sister chromatid exchange (SCE) induction and a microdosimetric assessment of the fraction of cell nuclei exposed to DU-induced alpha particles was determined. (A) Frequency distribution of SCE formation, measured as described in Materials and Methods. (B) Frequency distribution of nuclei hit by an alpha particle; microdosimetric assessment was determined using a Monte Carlo computer simulation based on measured levels of intracellular and extracellular uranium as described in the methods. F(hit) = 1.4 × 10^{-3}%.

in SCEs (lead acetate, 20 μM: 8.9 SCE/cell; $NiSO_4$, 20 μM: 11.4 SCE/cell).

Using a standard uranium analysis technique, KPA (*15*), the amount of uranium per cell following a 24-hr treatment with 10 μM DU-UO_2^{2+} was determined to be 1.8 (± 0.15) × 10^{-6} ng/cell with the average intercellular concentration being 2 μM.

To examine the stochastic fluctuations of alpha particle hits and energy deposition in the cell nuclei, microdosimetric methods using Monte Carlo computer simulations were applied (Figure 1B). The computer code, designed by Humm (*14*) to predict cell inactivation by internal alpha emitters, was modified to correspond to the experimental conditions as described in Materials and Methods. The trajectory of each alpha particle was calculated using vector analysis to determine whether it would hit a nucleus. The energy transferred to the nucleus was calculated by determining the residual energy retained by the alpha particle as it penetrated the nucleus. The calculations determined that only 0.0014% of the nuclei were hit and that the mean specific energy received by those cells was approximately 17 cGy. The results, plotted as a frequency distribution, are shown in Figure 1B.

Transformation of HOS cells by DU-UO_2^{2+}: comparison to $NiSO_4$ and lead acetate. To assess for morphological cell transformation, the standard focus formation assay described by Reznikoff et al. (*10*) and Hill et al. (*12*) was used. After exposure to DU-UO_2^{2+}, a morphological change in HOS cells was observed (Fig. 2). HOS cells exhibit a flat epithelial-like morphology and appear to grow in a monolayer (Fig. 2A). In contrast, after treatment with DU-UO_2^{2+} and weekly changes of nutrient medium for 5 weeks, diffuse type II foci appeared (Fig. 2B). The morphology of the focus is distinctly different from the surrounding cells (Fig. 2B), although the focus does not exhibit the "piled up" appearance seen in transformed $C3H10T_{1/2}$ cells (*10*). Table 1 shows measured values for the transformation frequencies (normalized per surviving cell) for HOS cells treated with DU-UO_2^{2+} (10 μM). The transforming abilities of $NiSO_4$ and lead acetate have been shown previously (*8,16*) but are repeated here to allow for a quantitative comparison to the DU compound. The data demonstrate that treatment with DU-UO_2^{2+} resulted in a transformation frequency of 40.2 × 10^{-4}, which is a 9.6 (± 2.8)-fold increase in transformation compared to untreated HOS cells. In comparison, the transformation frequencies induced by $NiSO_4$ and lead acetate treatment resulted in a 7.1 (± 2.1)- and 5.0 (± 1.6)-fold increase in transformation frequency compared to untreated cells.

Several foci were picked by cloning cylinders and expanded by mass culture to establish transformed clonal lines. Four DU-transformed clones (designated as DU1, DU2, DU3, and DU4) were selected for tumorigenic and growth analysis; a $NiSO_4$- and a lead acetate-transformed clone were also selected for similar analyses. A spontaneous focus arising from untreated HOS cells was also selected and expanded.

Biological characterization of the transformed phenotype. Alteration in growth control is critical to neoplastic transformation, and therefore the metal-transformed clones were further characterized by quantitative differences in growth properties associated with the neoplastic phenotype (e.g, saturation density and soft colony-forming efficiency). Additionally, to determine if cells transformed *in vitro* were capable of producing tumors in immunosuppressed mice, the nude mouse assay was used to test the tumorigenicity of DU-transformed cells (*9,10*). From Table 2 it can be seen that the saturation densities of DU-transformed cells were three to four times higher than that of the parental HOS cells. Data obtained for $NiSO_4$- and lead acetate-transformed cells were similar to that for DU. A comparison of the transformants' ability to grow in soft agar reveals that the DU transformants generated colonies within 1 week, with colony-forming efficiencies of 32–51%; the plating efficiencies were somewhat lower for $NiSO_4$- or lead acetate-transformed cells. Parental HOS cells did not form colonies in soft agar (Table 2). We have previously shown that MNNG and EJ-*ras* transformants formed soft agar colonies whose size and frequency were comparable to those observed with these DU transformants (*9*).

Inoculation of athymic nude mice with DU transformants resulted in the development of animal tumors within 4 weeks. All of the DU transformed cell lines analyzed for tumorigenicity appeared to be highly tumorigenic because as few as 1 million DU-transformed cells developed progressively growing tumors within 4 weeks. Similarly, nude mice inoculated with $NiSO_4$ or lead acetate transformants also formed tumors (Table 2). In contrast, parental HOS cells injected into nude mice did not form any tumors during a period of 6 months after cell inoculation. Histological analysis indicates that the tumors formed by DU-transformed cells resemble a carcinoma characterized by an undifferentiated, sheetlike growth. Tumors were reestablished in tissue culture and confirmed as human; their resemblance to

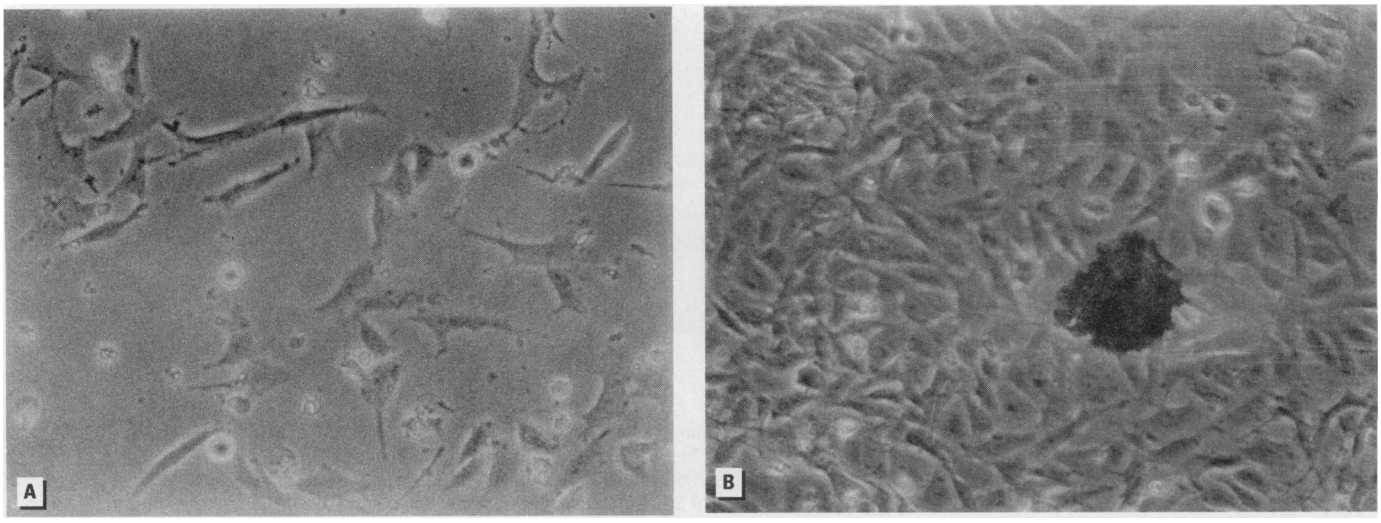

Figure 2. Morphology of HOS cells and focus formation after DU-UO_2^{2+} exposure. (A) Morphology of control HOS cells; phase contrast micrograph, (×40). (B) Focus formation in HOS cell; the edge of a focus of transformed cells is seen against a background of parental HOS cells with normal morphology (×40).

Table 2. Biological properties of human osteoblastlike cells transformed by depleted uranium-uranyl chloride, nickel sulfate, or lead acetate

Metal/clone designation	Saturation density (1×10^5 cells)[a]	Plating efficiency in soft agar (%)[a]	Nude mice with tumors[b]		SCE/cell (mean ± SE)
			5×10^6 cells	1×10^6 cells	
None/control	2.6	0	0/82	0/20	8.50 ± 0.06
DU-UO_2Cl_2/DU-1	7.9	51	8/19	6/12	18.53 ± 1.84
DU-UO_2Cl_2/DU-2	6.7	32	3/6	2/6	20.11 ± 2.02
DU-UO_2Cl_2/DU-3	8.2	47	4/6	2/6	21.01 ± 2.12
DU-UO_2Cl_2/DU-4	7.8	44	3/6	3/6	18.23 ± 1.88
$NiSO_4$/nickel-1	7.2	29	4/12	2/6	12.29 ± 1.19
$PbAc_2$/lead-1	6.5	19	1/10	ND	11.27 ± 1.02

Abbreviations: SCE, sister chromatid exchange; ND, not determined.
[a]Data represent three independent and identical experiments.
[b]Tumor latency was approximately 4 weeks.

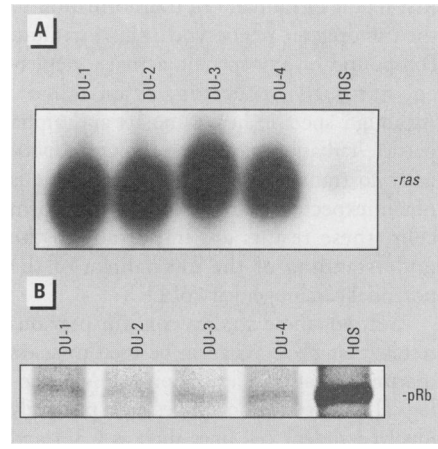

Figure 3. Analysis of K-*ras* expression and Rb protein production in parental HOS and DU-UO_2Cl_2-transformed clones. (A) *ras* Oncogene expression; Northern blot analysis of cytoplasmic RNA (20 µg) from DU-1, DU-2, DU-3, DU-4, and HOS. Hybridization was with a ^{32}P-labeled K-*ras* probe (*ras* transcripts were undetectable in HOS cells). Hybridization with ^{32}P-labeled actin was used to indicate that the relative amounts of RNA loaded into each lane were the same (data not shown). (B) Rb protein level; immunoprecipitation analysis of Rb protein from DU-1, DU-2, DU-3, DU-4, and HOS. Anti-pRb1 was used to capture cellular Rb protein containing ^{32}P.

the cells of origin was determined by karyological analysis (data not shown).

In contrast to the data presented in Figure 1A which demonstrate "acute" SCE elevation by DU, "persistent" cytogenetic changes, manifested as effects on the levels of SCEs per cell, were measured in the four transformed clones selected. Cytogenetic analysis of the DU-uranyl chloride-transformed clones revealed that all of the clones had a 2.14 (± 0.22)- to 3.47 (± 0.31)-fold higher level of SCE per cell compared to parental HOS cells (Table 2). The untreated, spontaneous HOS transformants did not exhibit a significant increase in SCE induction [1.07 (± 0.22)-fold increase] compared to parental HOS cells.

ras and pRb analysis in DU transformants. Neoplastic cell transformation is hypothesized to result from a multistep process involving activation of oncogenes and inactivation of tumor-suppressor genes (*17*). Both metal- and radiation-induced neoplastic transformation have been shown to be associated with genetic alterations in specific oncogenes and tumor-suppressor proteins, such as *ras* and pRb (*6,9*). Therefore, possible molecular changes in *ras* and pRb associated with DU-induced transformation were studied using the four DU-transformed cell lines. Northern blot analysis, shown in Figure 3A, revealed high levels of *ras* mRNA in each of the four DU clones tested. In contrast, the *ras* mRNA levels were undetectable in parental HOS. The amount of actin mRNA was similar in all clones tested (not shown). Heavy-metal–induced transformation (e.g., nickel) has been shown to cause a loss of phosphorylation of the retinoblastoma protein. We therefore used anti-pRb1 monoclonal antibodies to compare the phosphorylation of the pRb of the different DU-transformed cell lines to the parental cells by assessing the quantity of radioactive phosphate incorporated into the Rb protein. Each of the DU clones examined exhibited significantly lower amounts of ^{32}P incorporated into pRb relative to the parental HOS cells (Fig. 3B). The lack of phosphorylation of pRb could be a result of less protein available to phosphorylate, abnormalities of the cyclin-associated kinase systems responsible for phosphorylation of pRb, a mutation in the *Rb* gene, or a combination of these possibilities. Previous observations with nickel-transformed HOS cells demonstrated a mutation was induced in these transformants that affected the ability of the Rb protein to be phosphorylated and function normally (*6*).

Dose response: morphological transformation by UO_2Cl_2. To further evaluate the ability of DU-uranyl chloride to morphologically transform cells, increasing concentrations of DU were tested for their transforming ability. The results in Table 3 show that there is a DU concentration-dependent increase in transformation frequency. A transformed clone was selected from each concentration tested and expanded to mass culture. An examination of the selected transformants' ability to grow in soft agar reveals that the DU transformants generated large colonies (>0.5 mm) within 1 week with colony-forming efficiencies ranging from 33% to 53%. Inoculation of athymic nude mice with these DU transformants resulted in the development of tumors within 4 weeks.

Discussion

Our studies demonstrate for the first time that the malignant transformation of immortalized human cells can be achieved by exposure to the depleted uranium compound UO_2Cl_2. These transformants showed morphological changes and anchorage-independent growth in soft agar, induced tumors when transplanted into nude mice, and exhibited alterations in *ras* oncogene expression and pRb phosphorylation. Based on equivalent concentrations and metal toxicities, the magnitude of this DU-UO_2^{2+} transformation is comparable to that seen here for $NiSO_4$ and approximately twofold higher than that observed for lead acetate, both known transforming metals (*8,16*). Furthermore, DU-UO_2^{2+} caused a dose-dependent frequency in the transformation of HOS cells. To our knowledge, this is the

Table 3. Transformation potential of DU-uranyl chloride: dose response

Treatment	Concentration (µM)	Surviving fraction	Transformation frequency per survivor[a] $\times 10^{-4}$	Plating efficiency in soft agar (%)	Nude mice with tumors[b] (5×10^6 cells injected)
Control	0	1.0	4.2 ± 1.1	0	0/82
DU-UO_2Cl_2	10	0.95	40.2 ± 5.0	46	8/19
	25	0.84	51.1 ± 7.0	47	3/6
	50	0.25	108.9 ± 12.0	53	5/6
	100	0.10	125.6 ± 15.0	44	4/6
	250	0.02	99.4 ± 10.0	33	4/6

[a]The transformation data were analyzed similar to that in Table 1. Data are the mean ± standard error from three independent experiments involving approximately 500 plates/treatment. The average number of transformed foci per dish was computed from the proportion of dishes free of transformed colonies, *f*, by $\lambda = -\ln f$. Transformation frequency = λ/number of surviving cells per dish.
[b]Tumor latency was approximately 4 weeks.

first report of human cell transformation to the tumorigenic phenotype by any uranium compound of any specific activity (depleted, naturally occurring, or enriched). Although specific heavy metals and alpha particle radiation have been shown individually to transform cultured cells and it is not unexpected that DU could transform cells, these results are important to the understanding of the mechanism of the potential carcinogenicity of DU.

Second, these studies confirm previous results that HOS cells can be used to assess morphological transformation (*8*). Morphological transformation studies have primarily involved rodent cell lines such as C3H and 10T1/2, and to our knowledge this is only the second time that HOS cells have been used for an assessment of morphological transformation. These studies with DU demonstrate another step in understanding the transformation process of HOS cells.

The precise mechanism(s) by which DU-UO_2^{2+} induces transformation in HOS cells is unknown. The possibility that alterations in specific oncogenes (e.g., *ras*) and/or inactivation of tumor-suppressor genes (e.g., *p53*, *Rb*) are involved in the conversion of these cells to the malignant phenotype has been considered. HOS cells contain a mutation at codon 156 resulting in a mutated form of p53 protein, which is believed to be partially responsible for their immortalization (*18*). As neoplastic conversion is postulated to result from a multistep process involving cell immortalization and gene alterations (*17,19*), the transformation of immortalized HOS cells by DU-UO_2^{2+} to the malignant phenotype may involve other cellular oncogenes in this process. Our data demonstrate that the *ras* oncogene was activated in the transformation process induced by DU exposure. The *ras* oncogenes have been implicated in both chemically and radiation-induced animal tumors (*20–22*) and spontaneous human tumors (*23*) and may play a prominent role in the multistage conversion process.

Because others have demonstrated that nickel-induced morphological transformation of HOS cells can affect the *Rb* gene and its encoded protein (*6*), we examined the status of this tumor-suppressor protein in our DU-transformed clones. Changes in the phosphorylation of the *Rb* tumor-suppressor gene-encoded protein in the DU-transformed clones were observed. The *Rb* gene has been shown to be mutated or inactivated in a broad spectrum of human tumors, including retinoblastoma, osteosarcoma, lung cancer, and breast cancer, and appears to be important in human carcinogenesis; furthermore, the inactivation of the *Rb* may be involved in the molecular mechanism of carcinogenesis of human osteoblasts (*24*). Recent *in vitro* studies with nickel-transformed HOS cells suggested that nickel exposure induced a mutation in the *Rb* gene that resulted in an alteration in the function of the Rb protein (*6*). It appears from our data that transformation of HOS cells by DU-UO_2^{2+} results from a conversion process which also involves activation of tumor-promoting gene(s) and/or alterations in tumor-suppressor proteins, including *ras*, *p53*, and *Rb*.

Without evidence that DU-UO_2^{2+} directly affects the DNA, we can only speculate about the mechanism(s) by which DU-UO_2^{2+} ultimately affects the *ras* gene and the Rb protein. The nature of this mechanism may involve direct damage to the DNA and to DNA repair processes. Transforming metals such as nickel can induce SCEs (*25*) and have been shown to directly damage DNA (*26*), whereas others such as lead acetate do not directly affect the genetic material and may induce transformation via an indirect mechanism such as changes in DNA conformation or enzymatic disturbances (*16*). An elevation in SCE levels has also been observed as the result of inhibition of DNA replication, rather than by direct damage of chromosomes (*25*). Our observation of an elevation in the level of SCE per cell, while consistent with these concepts, cannot distinguish between them. The mechanism of action at the genomic level for DU-induced transformation has not been determined and awaits further investigation; it is possible that DU induces transformation via mechanisms similar to those observed for nickel or lead, or by other by unknown mechanisms.

Elucidation of the mechanism by which DU transforms cells is further complicated by the concurrent exposure to both the chemical (heavy metal) component and the radiological (alpha particle) components from DU. The chemical toxicity of uranium, based on animal and epidemiology studies, is well known (*27*) and is believed to be responsible for cytogenetic damage observed in the lymphocytes from men occupationally exposed to insoluble uranium (*28*), but has not been linked to uranium carcinogenesis. However, our results provide evidence that the chemical/metal toxicity of DU plays a significant role in its ability to morphologically transform human cells. It is interesting to speculate that the observed chemical toxicity of DU-UO_2^{2+} may be attributed to the radiomimetic property of uranyl ions to act as a transition metal to produce free radicals via a Fenton-like reaction (*29*), similar to those chemical properties generally attributed to iron-II, copper-I, and recently demonstrated for plutonium by Claycamp and Luo (*30*). DNA is an effective chelator of metal ions, which suggest the possibility of a metal-mediated, site-specific free radical damage (*31*).

Increased lung cancer risks in uranium miners and uranium milling workers have been attributed to exposure to the alpha particle emitter radon and its daughter products (*1,32*). In our study with DU exposures *in vitro*, the biological effect from the radiological component may be significantly reduced since so few cells (0.0014%) are actually hit by alpha-particle emissions (1 alpha particle traversal/cell hit). Therefore, in our study, the defining question is whether the alpha particle dose distribution and its track could effectively produce a change in that target cell that would induce or promote morphological transformation. Preliminary data using an alpha particle microbeam have demonstrated that one alpha particle traversal of a cell is not enough to induce morphological transformation (*33*). Although these data from Miller's laboratory and our results argue for a negligible role for alpha radiation in the DU-UO_2^{2+}-induced transformation, low levels of exposure to alpha radiation have been shown to induce genetic changes (*34*) and chromosomal instability (*35*) in the progeny of alpha-irradiated cells. The involvement of transmitted genetic instability in the transformation process is not fully understood and cannot be ignored because it could possibly be involved in the DU-UO_2^{2+}-induced transformation. Whether by radiation or chemical mechanism, DU-UO_2^{2+} exposure is consistent with the generally accepted features associated with neoplastic transformation of cells by radiation or metal exposure including formation of sister chromatid exchanges (*31,36,37*) and genomic instability manifested as gene alterations (*6,36,38*).

In summary, we have used a model system of *in vitro* human osteoblast cells exposed for 24 hr to DU-uranyl chloride (10 μM), nickel sulfate (10 μM), or lead acetate (10 μM) to assess relative transforming potential of DU in an effort to better understand the potential health risks from long-term exposure to internalized DU. Despite the well-known low solubility of uranyl compounds, we found cellular uptake of uranium consistent with other transuranic compounds (*39*). As expected from the prompt chemical toxicity of heavy metal exposure, the levels of SCEs were elevated in DU-UO_2^{2+}-treated cells. Microdosimetry studies demonstrate that few ($<1.4 \times 10^{-3}$%) cells are actually hit by alpha particles emitted from DU. This argues for a negligible role for radiation effects from DU-UO_2^{2+} exposure. DU-UO_2^{2+} appears to be 1.34 (± 0.24)- and 1.91 (± 0.42)-fold more potent that nickel sulfate and lead acetate, respectively, in inducing an elevation

in neoplastic cell transformation frequency *in vitro* at equivalent concentrations. Hence, DU-UO_2^{2+} appears to have transforming ability slightly greater than that of many other trace heavy metals, which also induce neoplastic cell transformation *in vitro*, as well as cause tumor formation in animals (*40*). While additional animal studies are needed to address the effect of protracted exposure and tumor induction *in vivo*, the implication from our model system study is that the risk of neoplastic induction from internalized DU exposure may be similar to other biologically reactive and carcinogenic heavy metal compounds such as lead and nickel.

References and Notes

1. NRC. Biological Effects of Ionizing Radiation (BEIR) IV. Health Risks of Radon and Other Internally Deposited Alpha-Emitters. NRC Committee on the Biological Effects of Ionizing Radiation. Washington, DC:U.S. National Research Council, 1988.
2. Danesi ME. Kinetic Energy Penetrator Long Term Strategy Study (abridged). Picatinny, NJ:US Army Armament Munitions and Chemical Command, Picatinny Arsenal, 1990.
3. U.S. Army Environmental Policy Institute. Health and Environmental Consequences of Depleted Uranium Use in the U.S. Army. Rpt no 1995. Atlanta, GA:U.S. Army Environmental Policy Institute, 1995.
4. Wrenn ME, Durbin PW, Howard B, Lipsztein J, Rundo J, Still ET, Willis D. Metabolism of ingested U and Ra. Health Phys 48:601–633 (1985).
5. Patierno SR, Banh D, Landolph JR. Transformation of C3H/10T1/2 mouse embryo cells to focus formation and anchorage independence by insoluble lead chromate but not soluble calcium chromate: relationship to mutagenesis and internalization of lead chromate particles. Cancer Res 48:5280–5288 (1988).
6. Lin X, Dowjat K, Costa M. Nickel-induced transformation of human cells causes loss of the phosphorylation of the retinoblastoma protein. Cancer Res 54: 2751–2754 (1994).
7. Lin X, Costa M. Transformation of human osteoblasts to anchorage-independent growth by insoluble nickel particles. Environ Health Perspect 102(suppl 3):289–292 (1994).
8. Rani AS, Qu D, Sidhu MK, Panagakos F, Shah V, Klein KM, Brown N, Pathak S, Kumar S. Transformation of immortal, non-tumorigenic osteoblast-like human osteosarcoma cells to the tumorigenic phenotype by nickel sulfate. Carcinogenesis 14:947–953 (1993).
9. Miller AC, Kariko K, Myers CE, Clark EP, Samid D. Increased radioresistance of EJ*ras*-transformed human osteosarcoma cells and its modulation by lovastatin, an inhibitor of $p21^{ras}$ isoprenylation. Int J Cancer 53:302–307 (1993).
10. Reznikoff CA, Bertram JS, Brankow DW, Heidelberger C. Quantitative and qualitative studies of chemical transformation of cloned C3H mouse embryo cells sensitive to postconfluence inhibition of cell division. Cancer Res 33:3239–3249 (1973).
11. IARC/NCI/EPA Working Group. Cellular and molecular mechanisms of cell transformation and standardization of transforming assays of established cell lines for the prediction of carcinogenic chemicals: overview and recommended protocols. Cancer Res 45:2395–2399 (1985).
12. Hill CK, Buonaguro FM, Myers CP, Han A, Elkind MM. Fission-spectrum neutrons at reduced dose rates enhance neoplastic transformation. Nature 298:67–69 (1982).
13. Perry P, Wolff S. New giemsa method for differential staining of sister chromatids. Nature 251:156–158 (1974).
14. Humm JL. A microdosimetric model of astatine-211 labeled antibodies for radioimmunotherapy. Int J Radiat Oncol Biol Phys 13:1767–1777 (1987).
15. Brina R, Miller AG. Direct detection of trace levels of uranium by laser-induced kinetic phosphorimetry. Anal Chem 64:1413–1418 (1992).
16. Zelikoff JT, Li JH, Hartwig A, Wang XW, Costa M, Rossman TG. Genetic toxicology of lead compounds. Carcinogenesis 9:1727–1734 (1988).
17. Barrett JC. Mechanisms of multistep carcinogenesis and carcinogen risk assessment. Environmental Health Perspectives 100:9–20 (1993).
18. Romano JW, Ehrhart JC, Duthu A, Kim CM, Appella E, May P. Identification and characterization of a p53 gene mutation in a human osteosarcoma cell line. Oncogene 4:1483–1488 (1989).
19. Rhim JS, Jin S, Jung M, Thraves PJ, Kuettel MR, Webber MM, Hokku B. Malignant transformation of human prostate epithelial cells by N-nitroso-N-methylurea. Cancer Res 57:576–580 (1997).
20. Cooper GM. Cellular transforming genes. Science 218: 801–806 (1982).
21. Guerrero I, Villasante A, Corces V, Pellicer A. Radiation-induced lymphoma in mouse. Science 225:1159–1162 (1984).
22. Sawey MJ, Hood AT, Burns FJ, Garte SJ. Radiation-induced lymphoma in mouse. Mol Cell Biol 7:932–935 (1987).
23. Weinberg RA. Tumor suppressor genes. Science 254:1138–1146 (1991).
24. Roarty JD, McLean IW, Zimmerman LE. Incidence of second neoplasms in patients with bilateral retinoblastoma. Ophthalmology 95:1583–1587 (1988).
25. Pleskach NM, Andriadze MI, Mikhelson VM, Zhestyanikov VD. Sister chromatid exchanges and inhibition of DNA synthesis in irradiated human cells. Acta Biology Hungary 41:209–213 (1990).
26. Sen P, Costa M. Induction of chromosomal damage in Chinese hamster ovary cells by soluble and particulate nickel compounds: preferential fragmentation of the heterochromatic long arm of the X-chromosome by carcinogenic crystalline NiS particles. Cancer Res 45:2320–2325 (1985).
27. Domingo JL. Chemical toxicity of uranium. TEN 2:3:46–50 (1995).
28. Martin F, Earl R, Tawn EJ. A cytogenetic study of men occupationally exposed to uranium. Br J Ind Med 48:98–102 (1991).
29. Hamilton MM, Ejnik JW, Carmichael AJ. Uranium recations with hydrogen peroxide studied by EPR-spin trapping with DMPO. J Chem Soc Perkin Trans 2:2491–2494 (1997).
30. Claycamp HG, Luo D. Plutonium-catalyzed oxidative DNA damage in the absence of significant alpha-particle decay. Radiat Res 137:114–117 (1994).
31. Blakely WF, Fuciarelli AF, Wegher BJ, Dizdaroglu M. Hydrogen peroxide-induced base damage in deoxyribonuclei acid. Radiat Res 121:338–343 (1990).
32. Vahakangas KH, Samet JM, Metcalf RA, Welsh JA, Bennett WP, Lane DP, Harris CC. Mutations of p53 and *ras* genes in radon-associated lung cancer from uranium miners. Lancet 339:576–580 (1992).
33. Miller RC, Randers-Pehrson G, Brenner DJ, Hall EJ, Geard CR. Microbeams and cellular changes: single particle induced oncogenic transformation. In: Proceedings of Microbeam Probes of Cellular Response, 9–11 May 1997, New York.
34. Nagasawa H, Little JB. Induction of sister chromatid exchanges by extremely low doses of alpha-particles. Cancer Res 52:6394–6396 (1992).
35. Kadhim MA, Macdonald DA, Goodhead DT, Lorimore SA, Marsden SJ, Wright EG. Transmission of chromosomal instability after plutonium alpha-particle irradiation. Nature 355:738–744 (1992).
36. Morgan WF, Day JP, Kaplan MI, McGhee EM, Limoli CL. Genomic instability induced by ionizing radiation. Radiat Res 146:247–258 (1996).
37. Christie NT, Costa M. Chromosomal alterations in cell lines induced by nickel sulfide. Biol Trace Elem Res 5:55–71 (1983).
38. Manti L, Jamali M, Prise KM, Michael BD, Trott K-R. Genomic instability in chinese hamster cells after exposure to X rays or alpha particles of different mean linear energy transfer. Radiat Res 147:22–28 (1997).
39. Zidenberg-Cherr S, Parks NJ, Keen CL. Tissue and subcellular distribution of bismuth radiotracer in the rat: considerations of cytotoxicity and microdosimetry for bismuth radiopharmaceuticals. Radiat Res 111:119–129 (1987).
40. Sunderman FW. Recent advances in metal carcinogenesis. Ann Clin Lab Sci 14:93–122 (1984).

THE EHIS PUTS EVEN MORE ENVIRONMENTAL HEALTH INFORMATION RIGHT AT YOUR FINGERTIPS!

NATIONAL LIBRARY OF MEDICINE

EHIS articles contain convenient **links to PubMed**—the National Library of Medicine's free on-line search service of more than 9 million citations! Search MEDLINE and Pre-MEDLINE (including links to other online journals and databases) for information directly related to each EHIS article's topic!

Subscribe to the EHIS today at: http://ehis.niehs.nih.gov/